

LETTERS

Preserving noble gases in a convecting mantle

Helge M. Gonnermann¹ & Sujoy Mukhopadhyay²

High $^3\text{He}/^4\text{He}$ ratios sampled at many ocean islands are usually attributed to an essentially undegassed lower-mantle reservoir with high ^3He concentrations^{1–4}. A large and mostly undegassed mantle reservoir is also required to balance the Earth's ^{40}Ar budget, because only half of the ^{40}Ar produced from the radioactive decay of ^{40}K is accounted for by the atmosphere and upper mantle⁵. However, geophysical^{6,7} and geochemical observations⁸ suggest slab subduction into the lower mantle, implying that most or all of Earth's mantle should have been processed by partial melting beneath mid-ocean ridges and hotspot volcanoes. This should have left noble gases in both the upper and the lower mantle extensively outgassed, contrary to expectations from $^3\text{He}/^4\text{He}$ ratios and the Earth's ^{40}Ar budget. Here we suggest a simple solution: recycling and mixing of noble-gas-depleted slabs dilutes the concentrations of noble gases in the mantle, thereby decreasing the rate of mantle degassing and leaving significant amounts of noble gases in the processed mantle. As a result, even when the mass flux across the 660-km seismic discontinuity is equivalent to approximately one lower-mantle mass over the Earth's history, high ^3He contents, high $^3\text{He}/^4\text{He}$ ratios and ^{40}Ar concentrations high enough to satisfy the ^{40}Ar mass balance of the Earth can be preserved in the lower mantle. The differences in $^3\text{He}/^4\text{He}$ ratios between mid-ocean-ridge basalts and ocean island basalts, as well as high concentrations of ^3He and ^{40}Ar in the mantle source of ocean island basalts⁴, can be explained within the framework of different processing rates for the upper and the lower mantle. Hence, to preserve primitive noble gas signatures, we find no need for hidden reservoirs or convective isolation of the lower mantle for any length of time.

The requirement of a ^3He - and ^{40}Ar -rich reservoir provides the strongest arguments for a relatively undegassed lower mantle^{1–3,5,9}. However, seismological observations of plate subduction into the lower mantle^{6,7} appear to be inconsistent with a relatively undegassed lower mantle. To reconcile the high $^3\text{He}/^4\text{He}$ ratios observed in ocean island basalts (OIBs) with the expectation of a processed and outgassed lower-mantle source, residues of mantle melting^{10,11}, depleted in uranium and thorium relative to ^3He , have been suggested to carry the high $^3\text{He}/^4\text{He}$ signatures. However, the preservation of high $^3\text{He}/^4\text{He}$ ratios in residues of mantle melting is apparently inconsistent with recently determined noble gas partition coefficients¹². Because helium is nevertheless incompatible, the low concentrations in residual mantle require convective isolation of the plume source over most of the Earth's lifetime. Convective isolation over geologically long periods (>1 Gyr) has also been suggested in other models for the evolution of helium in the OIB mantle source¹³.

By contrast, we find that the solution to the apparent discrepancy between an outgassed lower mantle and high concentrations of primordial ^3He in the lower mantle lies in the ubiquitous process of recycling and mixing of degassed slabs back into the mantle. During partial melting, noble gases behave incompatibly and strongly partition into the basaltic melt, which forms the ocean crust and leaves the residual mantle severely depleted of noble gases.

However, ocean crust is extensively degassed and when slabs, comprised of the degassed oceanic crust and residual mantle, are recycled back into the mantle, they contain negligible mantle-derived helium¹⁴. Mixing of these ^3He -depleted slabs with ambient mantle will dilute average helium concentrations in the mixed mantle assemblage. Because the rate at which noble gases are lost from the mantle is proportional to the gas concentration within the mantle being processed by melting, the monotonically decreasing noble gas concentrations in the evolving mixed mantle assemblage will result in a decreasing outgassing rate at any given processing rate (Fig. 1). In the simplest case of slabs mixing instantaneously with mantle, the average concentration of a primordial noble gas, such as ^3He , in a convectively mixed mantle assemblage evolves as

$$\bar{C}(t) = e^{(f-1)qt} \approx e^{-qt} \quad (1)$$

Here $\bar{C} = C/C_0$, with C the concentration in the mantle reservoir at time t and C_0 the initial concentration, $f \approx 0$ is the fraction of a given noble gas that remains in the mantle residue after melting and q is the rate at which the mantle reservoir is processed through melting over 4.5 Gyr. Present-day concentrations are given by e^{-N} , where N is the number of times the reservoir has been processed through partial melting over 4.5 Gyr. This simple analytic expression demonstrates that even after one reservoir mass has undergone processing by partial melting ($N = 1$), $\sim 37\%$ of primordial ^3He is retained in the reservoir (Fig. 2, dashed line).

Mixing of subducted slabs with ambient mantle is not instantaneous, but is thought to have an exponential dependence on time^{15,16}. Convective motions stretch and juxtapose recycled slab and ambient mantle at increasingly smaller length scales over a characteristic mixing time, τ , which may range between a few hundred million years to a few billion years^{15–17}. Partial melting of this mixed mantle assemblage will extract noble gases in proportion to their average concentrations within the melting region. If mixing of recycled slab to length scales that are smaller than the melting region occurs at a rate proportional to $qe^{-s/\tau}$, where s is the time after slab formation, then (Methods)

$$\bar{C} = \exp \left[\frac{1}{q\tau - 1} \ln(1 - q\tau + q\tau e^{-t/\tau}) + \frac{qt}{q\tau - 1} \right] \quad (2)$$

Figure 2 shows that for any reasonable estimate of τ , at least 30% of primordial ^3He will be retained in a mantle reservoir even after one reservoir mass has been processed. Therefore, preserving high concentrations of ^3He in the Earth's lower mantle does not require convective isolation or inefficient mixing. Because incompatible trace elements have been preferentially sequestered in the continental crust, a processed ^3He -rich lower mantle should have depleted strontium and neodymium isotopic characteristics relative to compositions of bulk silicate Earth (BSE), consistent with the mantle component that carries the signature of high $^3\text{He}/^4\text{He}$ ratios in OIBs (the focus zone, or FOZO)^{13,18}. A mantle reservoir that has been processed repeatedly

¹Department of Earth Science, Rice University, Houston, Texas 77005, USA. ²Department of Earth and Planetary Sciences, Harvard University, Cambridge, Massachusetts 02138, USA.

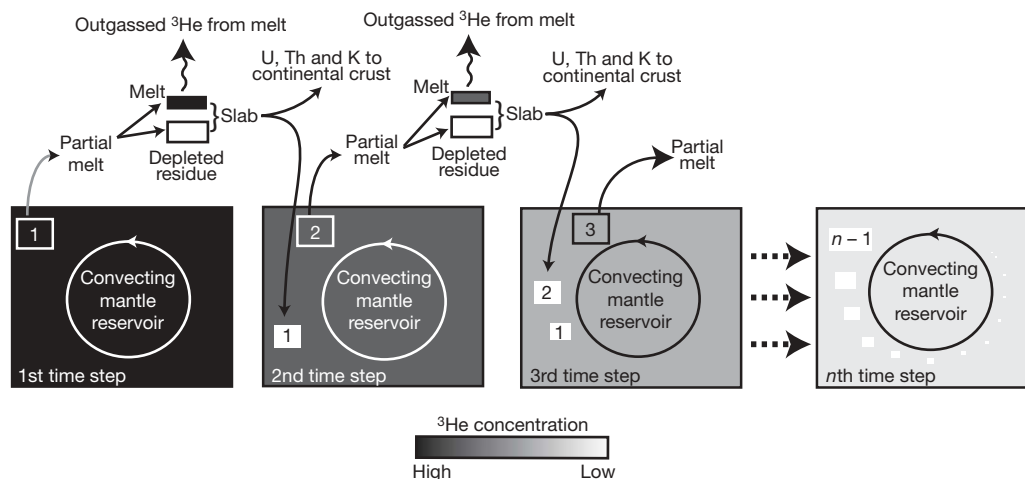


Figure 1 | Conceptual model of mantle degassing. Idealized processing of a mantle reservoir through partial melting, shown schematically in discrete time steps. Uranium, thorium, potassium and the noble gases (^3He shown here) are incompatible and partition preferentially into the basaltic melt phase, leaving a depleted mantle residue. The basaltic melt degasses before it solidifies to form ocean crust, but remains enriched in incompatible elements. Ocean crust plus mantle residue comprise slab, which is subducted back into the mantle. During subduction, any residual helium is lost from

over the Earth's history ($N = 2-4$) is considerably more degassed, but, depending on τ , can still contain a few per cent primordial ^3He . This is consistent with the $^3\text{He}/^4\text{He}$ of the mid-ocean-ridge basalt (MORB) mantle source.

To test under what conditions mixing of noble-gas-depleted slabs back into the mantle is quantitatively consistent with observed $^3\text{He}/^4\text{He}$ ratios, ^3He concentrations and the Earth's ^{40}Ar budget, we use geochemical reservoir modelling¹⁹⁻²¹ (see Methods and Supplementary Information for a detailed description). We model two mantle reservoirs corresponding in mass to the Earth's upper mantle (MORB source) and lower mantle (OIB source), respectively. We start with both the upper and the lower mantle being homogeneous and having BSE compositions (Fig. 1). The reservoirs degas by processing through partial melting near the Earth's surface to

the slab¹⁴ and some of the uranium, thorium and potassium are extracted from the slab and incorporated into the continental crust. The noble-gas-depleted slab eventually becomes mixed in with the remaining mantle reservoir over a characteristic timescale, τ . Because of slab recycling, ^3He concentrations in the mixed mantle assemblage decrease over time and the rate of ^3He degassing at a given processing rate decreases monotonically. Consequently, a significant fraction of ^3He is retained, despite extensive processing.

produce oceanic crust and an underlying residual mantle, which together comprise the slab. We assume that the ocean crust loses all helium and argon before being subducted back into the mantle, which introduces chemical heterogeneity into the mantle. The recycled slabs mix with the ambient mantle (Fig. 1) on a characteristic timescale, τ , which can differ between the upper and the lower mantle and is allowed to vary from 0–4 Gyr. Thus, the lower- and upper-mantle reservoirs evolve from a homogeneous reservoir to one that contains a well-mixed assemblage and unmixed slabs (Fig. 1), the amount of which depends on τ .

In our model, we assume that only the mixed mantle assemblage undergoes processing by partial melting and we allow the fraction of slab that subducts into the lower mantle to vary from zero to one. The mass flux of slab into the lower mantle is balanced by a subsequent

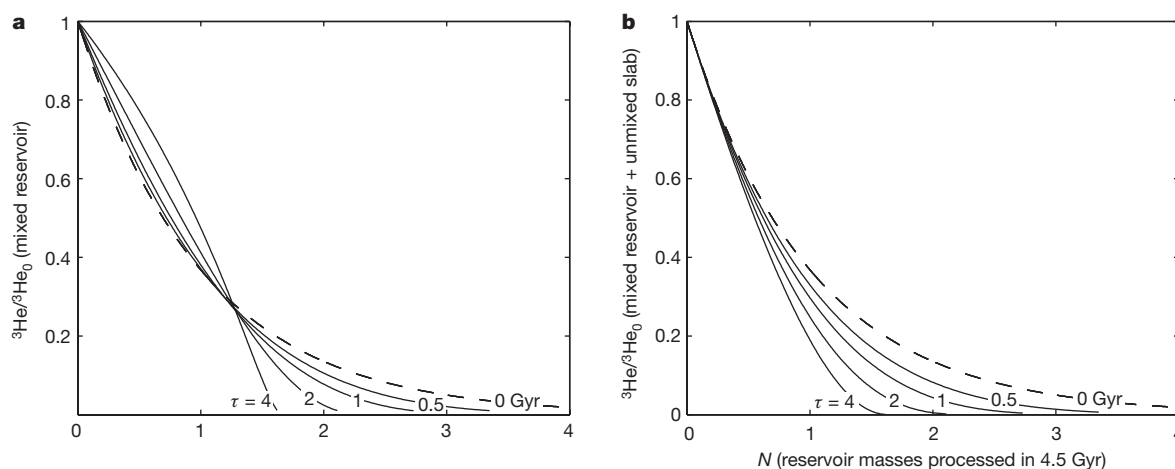


Figure 2 | Primordial noble gas concentration in the processed mantle reservoir. **a**, Concentration of ^3He in the mixed mantle reservoir after 4.5 Gyr (normalized to the initial concentration, $^3\text{He}_0$), plotted as a function of the number of times the reservoir has been processed, N . Each curve corresponds to a given value of τ . The case of instantaneous mixing of slabs with the ambient mantle is represented by $\tau = 0$ Gyr, shown as the dashed curve. Even for values of τ greater than 1 Gyr, processing of a mantle reservoir at a rate of one reservoir mass over the Earth's history ($N = 1$) leads to the concentration of primordial noble gases in the mixed mantle reservoir being at least 30% of its initial value. By contrast, repeated

processing ($N \geq 2$) will result in significant degassing and primordial helium concentrations of about 1% of initial values. With the exception of the case in which $\tau = 0$ Gyr, the intersection of the curves with the horizontal axis ($^3\text{He}/^4\text{He} = 0$) represents the point at which the entire mantle reservoir consists only of unmixed slabs. We note that for $N < 1$ and large values of τ , little of the recycled slab has mixed back into the mantle. **b**, Same as in **a**, but for the entire mantle reservoir (mixed reservoir plus unmixed slab). Over a wide range of conditions, the total ^3He retained within a convecting mantle reservoir is a substantial fraction of the initial ^3He . Concentrations calculated using equations (1) and (2).

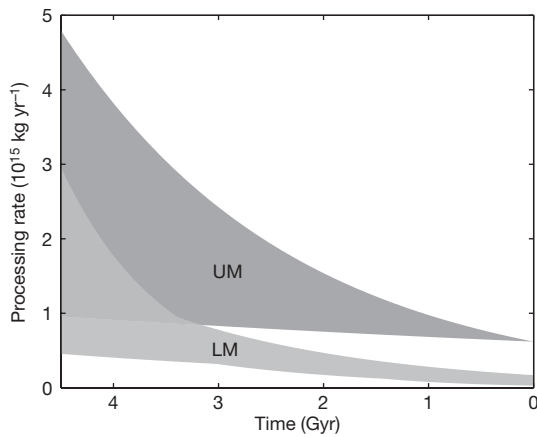


Figure 3 | Mantle processing rate. Range of instantaneous mantle processing rate as a function of time for the upper mantle (UM) and the lower mantle (LM), for models that meet geochemical constraints. The processing rate decreases exponentially in time to present-day processing rates beneath mid-ocean ridges ($7 \times 10^{14} \text{ kg yr}^{-1}$) for UM²⁶, and to plume flux estimates ($(2-20) \times 10^{13} \text{ kg yr}^{-1}$) for LM²⁷. The shaded areas represent the regions of overlap for individual curves; any kinks in the shaded areas are a consequence of intersecting curves.

return flow out of the lower mantle. This is either processed directly, by partial melting, presumably at hotspots and large igneous provinces, or a fraction of it is mixed into the upper mantle with only the remainder being directly processed. The residual mantle generated from partial melting of upwelling lower mantle can mix directly with the upper mantle or become part of the slab. We model a wide range of mantle processing rates that decrease exponentially in time¹⁵ to estimated present-day mid-ocean-ridge processing rates for the upper mantle and plume flux rates for the lower mantle (Fig. 3).

Within the framework of our model, we find that the high $^3\text{He}/^4\text{He}$ ratios measured in OIBs are entirely consistent with a lower-mantle source that has been depleted over the Earth's lifetime. Recycling of slabs into the lower mantle results in processing of 0.5–1 lower-mantle masses over the Earth's history, and the present day ^3He concentrations in the mixed regions of the lower mantle are consistent with estimates from OIB degassing models⁴ (Fig. 4). The well-mixed

lower-mantle assemblage has a non-primordial neodymium isotopic composition (Supplementary Information) and contains the high ^{40}Ar concentrations that are required to balance the Earth's ^{40}Ar budget. Hence, we find no argon concentration paradox⁵. The amount of upper mantle processed over the Earth's history falls within the range of 2.5–7.5 upper-mantle masses, consistent with a more depleted upper mantle. Characteristic mixing times for the lower mantle are up to ~ 2 Gyr and less than 1 Gyr for the upper mantle. Model results predict that at present $\sim 30\%$ of slabs subduct into the lower mantle with an average of $\sim 50\%$ over the Earth's history. Direct mixing of lower mantle with upper mantle comprises less than 10% of the lower-mantle flux across the 660-km seismic discontinuity.

These results can be interpreted to indicate that over much of the Earth's history, slab subduction into the lower mantle^{6,7} is balanced by a lower-mantle return flow that rises with little mixing through the upper mantle to shallow depths where partial melting results in outgassing and produces large igneous provinces, hotspot volcanoes or plume-influenced MORBs. Consequently, there is limited direct input of noble gases from the lower to the upper mantle. Over the Earth's history, the lower-mantle return flow results in a mass exchange of approximately one lower-mantle mass across the 660-km discontinuity. Hence, the noble gas view suggests that up to 50% of slabs produced over the Earth's history have subducted into the lower mantle across a 660-km discontinuity that opposes unfettered mixing between the upper and the lower mantle. This is consistent with the seismic evidence that slab stagnation is common in the transition zone²² and with the significantly different spatial patterns of shear-wave velocity anomalies on either side of the 660-km discontinuity, which indicate limited direct coupling of flow between the upper and the lower mantle^{23,24}.

From our analytic treatment (Fig. 2) and geochemical reservoir modelling (Fig. 4), we find that the recycling and mixing of outgassed slabs allows the preservation of high noble gas concentrations in a processed mantle reservoir. We find no noble gas requirements for convective isolation or hidden reservoirs in the lower mantle. The differences in measured $^3\text{He}/^4\text{He}$ ratios, as well as helium and argon concentrations, between MORBs and OIBs can be explained by an upper mantle that has been processed several times with respect to its mass, whereas the lower mantle has been processed approximately

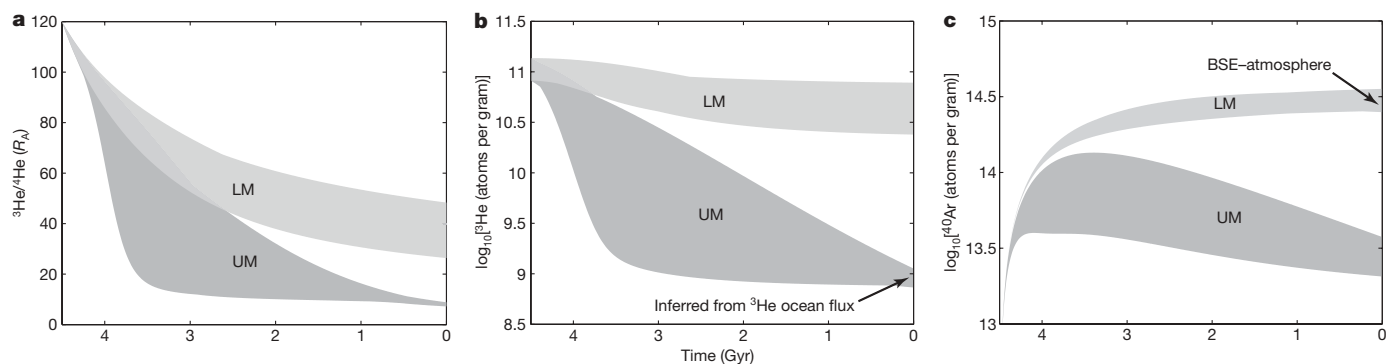


Figure 4 | Results from geochemical reservoir modelling. Initial $^3\text{He}/^4\text{He}$ ratios are $120R_A$, where R_A denotes the atmospheric $^3\text{He}/^4\text{He}$ ratio²⁸. The initial ^3He concentration is $(7.5-15) \times 10^{10}$ atoms per gram, within the range of previous estimates^{3,26}, and there is no primordial ^{40}Ar . Uranium, thorium and potassium concentrations at 4.5 Gyr are BSE values for both UM and LM (^{238}U , 40 p.p.b.; ^{235}U , 12 p.p.b.; ^{232}Th , 95 p.p.b.; ^{40}K , 327 p.p.b.). The shaded areas represent model simulations where present-day upper-mantle $^3\text{He}/^4\text{He}$ ratios are $(8.5 \pm 0.5)R_A$; uranium and potassium concentrations are within 3.2–5.4 p.p.b. and 50–68.4 p.p.m., respectively^{29,30}; lower-mantle $^3\text{He}/^4\text{He}$ ratios are larger than $35R_A$; the predicted ^3He outgassing rate at mid-ocean ridges is within 75–100% of the estimated ^3He flux to the oceans³¹ ($1,060 \text{ mol yr}^{-1}$); and approximately 40–60% of radiogenic ^{40}Ar produced over 4.5 Gyr still resides within the Earth's mantle. **a**, Modelled evolution in

$^3\text{He}/^4\text{He}$ ratios in the mixed UM and LM reservoirs, as a function of time. **b**, The resultant range and evolution of ^3He in the mantle reservoirs. **c**, Predicted range and evolution of radiogenic ^{40}Ar for zero primordial ^{40}Ar . Despite processing of up to one LM mass, present-day ^{40}Ar in the LM ranges between approximately 2.5×10^{14} and 3.6×10^{14} atoms per gram, which accounts for 40–60% of the ^{40}Ar produced over the Earth's history, with most of the remaining ^{40}Ar outgassed to the atmosphere. This is consistent with the Earth's atmospheric ^{40}Ar budget. Because of repeated processing, the ^{40}Ar concentration of the UM is substantially lower, ranging between approximately 2.1×10^{13} and 3.8×10^{13} atoms per gram. This is within the range of values predicted from the measured ^3He flux to the Earth's oceans, assuming a $^3\text{He}/^4\text{He}$ ratio of about $8.5R_A$ and a production ratio of three²⁸ for $^4\text{He}/^4\text{Ar}$.

once. A simple explanation for this is that the upper mantle is efficiently processed on timescales of 0.5–1 Gyr as a consequence of mid-ocean-ridge migration²⁵ and relatively low viscosity, whereas the lower mantle is inefficiently processed as a result of its higher viscosity and because mantle flow across the 660-km discontinuity is impeded^{22–24}.

High concentrations of ⁴⁰Ar and ³He and ³He/⁴He ratios of about 50R_A, noble gas characteristics that are normally attributed to a primitive mantle or hidden reservoirs, can be preserved in a convecting and processed lower mantle. Moreover, these noble gas characteristics are expected to be associated with depleted strontium and neodymium isotopic compositions, which are characteristic of the mantle component FOZO^{13,18} (Supplementary Information). Although FOZO is often thought of as an ancient mantle reservoir¹⁸, our modelling suggests that its noble gas signature can be attributed to a depleted mantle reservoir that has continuously evolved through slab recycling. A continuum of compositions between relatively well-mixed lower mantle assemblage (FOZO) and incompletely mixed recycled slabs is likely to produce the observed variability of ³He/⁴He ratios in OIBs.

METHODS SUMMARY

The free parameters in our geochemical reservoir model are the τ values for the upper and the lower mantle, mantle processing rates through time, rates of sequestration of uranium, thorium and potassium in the continental crust, the fraction of slab subducted into the lower mantle, the amount of direct mixing of the lower mantle with the upper mantle and the fraction of residual plume mantle that mixes directly with the upper mantle. We use Monte Carlo simulations in which free parameters are allowed to vary independently to determine their permissible range with respect to observational constraints. For each simulation, the mass balances for ³He, ⁴He, ⁴⁰Ar, uranium, thorium and potassium in the continental crust and in the well-mixed and unmixed slabs of the upper- and lower-mantle reservoirs are calculated as functions of time by numerical integration (see Methods and Supplementary Information for details). The model is constrained by a set of initial conditions (the initial ³He/⁴He ratio and the initial ³He, ⁴⁰Ar, uranium, thorium and potassium concentrations) and a set of present-day observations (the upper-mantle ³He concentration, the ³He/⁴He ratios and ⁴⁰Ar concentrations in the upper and the lower mantle, the upper-mantle processing rate as given by global ocean-crust production rate, lower-mantle processing rates as given by the plume mass flux and present-day uranium and potassium concentrations in the depleted MORB mantle). The vast majority of model runs do not meet the present-day observational constraints, and only successful runs that simultaneously satisfy all such constraints are shown in Fig. 4.

Full Methods and any associated references are available in the online version of the paper at www.nature.com/nature.

Received 8 December 2008; accepted 24 March 2009.

1. Kurz, M. D., Jenkins, W. J. & Hart, S. R. Helium isotopic systematics of oceanic islands and mantle heterogeneity. *Nature* **297**, 43–47 (1982).
2. Allègre, C. J., Staudacher, T. & Sarda, P. Rare-gas systematics: formation of the atmosphere, evolution and structure of the Earth's mantle. *Earth Planet. Sci. Lett.* **81**, 127–150 (1987).
3. Harper, C. L. & Jacobsen, S. B. Noble gases and Earth's accretion. *Science* **273**, 1814–1818 (1996).
4. Gonnermann, H. M. & Mukhopadhyay, S. Non-equilibrium degassing and a primordial source for helium in ocean-island volcanism. *Nature* **449**, 1037–1040 (2007).
5. Allègre, C. J., Hofmann, A. & O'Nions, K. The argon constraints on mantle structure. *Geophys. Res. Lett.* **23**, 3555–3557 (1996).
6. Grand, S. P., van der Hilst, R. D. & Widiyantoro, S. Global seismic tomography: a snapshot of convection in the Earth. *GSA Today* **7**, 1–7 (1997).
7. van der Hilst, R. D., Widiyantoro, S. & Engdahl, E. R. Evidence for deep mantle circulation from global tomography. *Nature* **386**, 578–584 (1997).

8. Hofmann, A. W., Jochum, K. P., Seufert, M. & White, W. M. Nb and Pb in oceanic basalts - new constraints on mantle evolution. *Earth Planet. Sci. Lett.* **79**, 33–45 (1986).
9. O'Nions, R. K. & Tolstikhin, I. N. Limits on the mass flux between lower and upper mantle and stability of layering. *Earth Planet. Sci. Lett.* **139**, 213–222 (1996).
10. Albarède, F. Time-dependent models of U-Th-He and K-Ar evolution and the layering of mantle convection. *Chem. Geol.* **145**, 413–429 (1998).
11. Parman, S. W. Helium isotopic evidence for episodic mantle melting and crustal growth. *Nature* **446**, 900–903 (2007).
12. Heber, V. S., Brooker, R. A., Kelley, S. P. & Wood, B. J. Crystal-melt partitioning of noble gases (helium, neon, argon, krypton, and xenon) for olivine and clinopyroxene. *Geochim. Cosmochim. Acta* **71**, 1041–1061 (2007).
13. Class, C. & Goldstein, S. L. Evolution of helium isotopes in the Earth's mantle. *Nature* **436**, 1107–1112 (2005).
14. Staudacher, T. & Allègre, C. J. Recycling of oceanic-crust and sediments—the noble-gas subduction barrier. *Earth Planet. Sci. Lett.* **89**, 173–183 (1988).
15. Allègre, C. J. & Turcotte, D. L. Implications of a two-component marble-cake mantle. *Nature* **323**, 123–127 (1986).
16. Coltice, N. & Schmalzl, J. Mixing times in the mantle of the early Earth derived from 2-D and 3-D numerical simulations of convection. *Geophys. Res. Lett.* **33**, doi:10.1029/2006GL027707 (2006).
17. Albarède, F. Rogue mantle helium and neon. *Science* **319**, 943–945 (2008).
18. Hart, S. R., Hauri, E. H., Oschmann, L. A. & Whitehead, J. A. Mantle plumes and entrainment - isotopic evidence. *Science* **256**, 517–520 (1992).
19. Jacobsen, S. B. & Wasserburg, G. J. Mean age of mantle and crustal reservoirs. *J. Geophys. Res.* **84**, 7411–7427 (1979).
20. Albarède, F. Radiogenic ingrowth in systems with multiple reservoirs: applications to the differentiation of the mantle-crust system. *Earth Planet. Sci. Lett.* **189**, 59–73 (2001).
21. Kellogg, J. B., Jacobsen, S. B. & O'Connell, R. J. Modeling the distribution of isotopic ratios in geochemical reservoirs. *Earth Planet. Sci. Lett.* **204**, 183–202 (2002).
22. Fukao, Y., Widiyantoro, S. & Obayashi, M. Stagnant slabs in the upper and lower mantle transition region. *Rev. Geophys.* **39**, 291–323 (2001).
23. Gu, Y. J., Dzierwowski, A. M., Su, W. & Ekström, G. Models of the mantle shear velocity and discontinuities in the pattern of lateral heterogeneities. *J. Geophys. Res.* **106**, 11169–11199 (2001).
24. Kustowski, B., Ekström, G. & Dzierwowski, A. M. Anisotropic shear-wave velocity structure of the Earth's mantle: a global model. *J. Geophys. Res.* **113**, doi:10.1029/2007JB005169 (2008).
25. O'Connell, R. J. & Hager, B. H. Ridge migration and mantle differentiation. *Eos* **61**, 373 (1980).
26. Porcelli, D. & Elliott, T. The evolution of He isotopes in the convecting mantle and the preservation of high ³He/⁴He ratios. *Earth Planet. Sci. Lett.* **269**, 175–185 (2008).
27. Kellogg, L. H. & Wasserburg, G. J. The role of plumes in mantle helium fluxes. *Earth Planet. Sci. Lett.* **99**, 276–289 (1990).
28. Graham, D. W. in *Noble Gases in Geochemistry and Cosmochemistry* (eds Porcelli, D., Ballentine, C. & Wieler, R.) 247–317 (Rev. Mineral. Geochem. Vol. 47, Mineralogical Society of America, 2002).
29. Workman, R. K. & Hart, S. R. Major and trace element composition of the depleted MORB mantle (DMM). *Earth Planet. Sci. Lett.* **231**, 53–72 (2005).
30. Boyet, M. & Carlson, R. W. A new geochemical model for the Earth's mantle inferred from ¹⁴⁶Sm–¹⁴²Nd systematics. *Earth Planet. Sci. Lett.* **250**, 254–268 (2006).
31. Farley, K. A., Maierreimer, E., Schlosser, P. & Broecker, W. S. Constraints on mantle ³He fluxes and deep-sea circulation from an oceanic general-circulation model. *J. Geophys. Res.* **100**, 3829–3839 (1995).

Supplementary Information is linked to the online version of the paper at www.nature.com/nature.

Acknowledgements We thank R. O'Connell, A. Dzierwowski, C. Langmuir, E. Hellebrand for discussions and D. Graham for a thorough review of the manuscript. H.M.G. was in part supported by the University of Hawaii, SOEST Young Investigator programme. S.M. was in part supported by US National Science Foundation grant EAR 0509721.

Author Contributions H.M.G. and S.M. together developed the ideas presented here. H.M.G. developed the geochemical reservoir model and performed the numerical modelling. H.M.G. and S.M. analysed the results and co-wrote the paper.

Author Information Reprints and permissions information is available at www.nature.com/reprints. Correspondence and requests for materials should be addressed to H.M.G. (helge@rice.edu) or S.M. (sujoy@eps.harvard.edu).

METHODS

Instantaneous mixing. The principal parameter that controls outgassing is the amount of processing that a given mantle reservoir undergoes over the Earth's history. If the depletion of a non-radiogenic noble gas is calculated for a mantle reservoir, under the assumption of 'instantaneous' recycling (instant mixing of the processed and degassed slab with the ambient reservoir), then the rate of change in concentration within this mixed reservoir is given by

$$\frac{dC}{dt} = -C(1-f)q$$

If q is a constant, integrating the equation gives us

$$C(t) = C_0 e^{-(1-f)qt}$$

For any feasible helium partition coefficient and melting model, and because helium is degassed from the oceanic crust, the $f=0$ approximation is reasonable, resulting in

$$C(t) \approx C_0 e^{-qt}$$

or

$$C(t = 4.5 \text{ Gyr}) \approx C_0 e^{-N}$$

Inefficient mixing. Mixing in the mantle is not likely to be instantaneous. An analytic formulation for a finite mixing time can be derived on the assumption that $f=0$ and that complete degassing of the melt fraction occurs. We assume that the fraction of slab produced at time s and remaining unmixed at time t is given by $e^{(s-t)/\tau}$, where τ is the characteristic mixing time. The cumulative mass of slab (normalized by the initial reservoir mass, M_0) produced at time t and remaining unmixed is therefore given by

$$\frac{M_s}{M_0} = \int_0^t q e^{(s-t)/\tau} ds = q\tau - q\tau e^{-t/\tau}$$

The complementary mass of the mixed mantle reservoir, M , is

$$\frac{M}{M_0} = 1 - \int_0^t q e^{(s-t)/\tau} ds = 1 - q\tau + q\tau e^{-t/\tau}$$

The rate of change in mass of the mixed reservoir at time t is given by

$$\frac{1}{M_0} \frac{dM}{dt} = -q e^{-t/\tau}$$

Using this expression, we find the rate of change in concentration of the mixed reservoir to be

$$\frac{dC}{dt} = \frac{C}{M} (q e^{-t/\tau} - q)$$

which upon integration results in

$$C = C_0 \exp \left[- \int \frac{q - q e^{-t/\tau}}{1 - \tau q + \tau q e^{-t/\tau}} dt \right]$$

or

$$C = C_0 \exp \left[\frac{qt + \ln(1 - \tau q + \tau q e^{-t/\tau})}{\tau q - 1} \right]$$

Mass-balance formulation for reservoir model. Please see Supplementary Fig. S4 for an illustration of the conceptual model. The mass lost from the mixed lower mantle at time step i is given by

$$\Delta M_{L,i} = Q_{L,i} \Delta t$$

and that lost from the upper mantle by

$$\Delta M_{U,i} = Q_{U,i} \Delta t$$

We define Δt as the duration of the time step and Q as the mass processing rate, given by

$$Q = Q_{\text{present}} e^{\alpha t}$$

Here t is time before present normalized to 4.5 Gyr and α is a parameter that varies independently for the upper and the lower mantle and for each simulation.

The mass of lower mantle that mixes with upper mantle at time step i is

$$\Delta M_{LU,i} = Q_{P,i} \Delta t$$

where $Q_{P,i}$ is the plume flux. The mass of residue generated from partial melting of plumes that mixes directly with upper mantle at time step i is

$$\Delta M_{PU,i} = x_{P,i} (1 - F) Q_{P,i} \Delta t$$

where x_P is the fraction of the residue generated from plume melting that mixes directly with the upper mantle and F is the melt fraction. The mass of ocean crust produced at time step i is

$$\Delta M_{O,i} = F(Q_{P,i} + Q_{U,i}) \Delta t$$

and the mass of residual mantle that becomes part of the slab at time step i is

$$\Delta M_{R,i} = (1 - F) ((1 - x_{P,i}) Q_{P,i} + Q_{U,i}) \Delta t$$

Ocean crust and residual mantle comprise slab and the mass of slab produced at time step i equals $M_{O,i} + M_{R,i}$. The mass of slab subducted into upper mantle at time step i is

$$\Delta M_{SU,i} = (1 - x_S) Q_{S,i} \Delta t$$

whereas that subducted into lower mantle is

$$\Delta M_{SL,i} = x_S Q_{S,i} \Delta t$$

Here x_S is the fraction of slabs subducted into the lower mantle and Q_S is the mass flux of subducting slab. The mass of slab subducted at time steps $j = 1, 2, \dots, i$ that becomes mixed with the mixed subreservoir of the upper mantle at time step i is

$$\delta M_{SU,i} = \sum_{j=1}^i \Delta M_{SU,j} (e^{-(i-j-1)\Delta t/\tau} - e^{-(i-j)\Delta t/\tau})$$

and the mass of slab subducted at time steps $j = 1, 2, \dots, i$ that becomes mixed with the mixed subreservoir of the lower mantle at time step i is

$$\delta M_{SL,i} = \sum_{j=1}^i \Delta M_{SL,j} (e^{-(i-j-1)\Delta t/\tau} - e^{-(i-j)\Delta t/\tau})$$

The concentrations of uranium, thorium, potassium, helium and argon as functions of time for each of the reservoirs follow directly from these mass balances. Additional considerations that are incorporated with these mass balances are radioactive decay of uranium, thorium and potassium and concurrent production of radiogenic ^4He and ^{40}Ar . These are based on the standard decay equations for these elements. The fractionation of radioactive elements and noble gases between melt (ocean crust) and residual mantle are based on the melting model discussed in Supplementary Information, with the added caveat that all noble gases are lost from the melt to the atmosphere and a fraction, x_C , of radioactive elements is sequestered from ocean crust into continental crust upon subduction.